Cardiovascular Research (2016) **110**, 346–358
doi:10.1093/cvr/cvw081

Prolyl hydroxylation regulates protein degradation, synthesis, and splicing in human induced pluripotent stem cell-derived cardiomyocytes

Andrea Stoehr[1], Yanqin Yang[2], Sajni Patel[3], Alicia M. Evangelista[1], Angel Aponte[3], Guanghui Wang[3], Poching Liu[2], Jennifer Boylston[1], Philip H. Kloner[1], Yongshun Lin[4], Marjan Gucek[3], Jun Zhu[2], and Elizabeth Murphy[1]*

[1]Systems Biology Center, National Heart, Lung, and Blood Institute, National Institutes of Health, Bethesda, MD, USA; [2]DNA Sequencing and Genomics Core, National Heart, Lung, and Blood Institute, National Institutes of Health, Bethesda, MD, USA; [3]Proteomics Core Facility, National Heart, Lung, and Blood Institute, National Institutes of Health, Bethesda, MD, USA; and [4]iPS Cell Core Facility, National Heart, Lung, and Blood Institute, National Institutes of Health, Bethesda, MD, USA

Received 15 December 2015; revised 24 March 2016; accepted 12 April 2016; online publish-ahead-of-print 19 April 2016

Time for primary review: 23 days

Aims Protein hydroxylases are oxygen- and α-ketoglutarate-dependent enzymes that catalyse hydroxylation of amino acids such as proline, thus linking oxygen and metabolism to enzymatic activity. Prolyl hydroxylation is a dynamic post-translational modification that regulates protein stability and protein–protein interactions; however, the extent of this modification is largely uncharacterized. The goals of this study are to investigate the biological consequences of prolyl hydroxylation and to identify new targets that undergo prolyl hydroxylation in human cardiomyocytes.

Methods and results We used human induced pluripotent stem cell-derived cardiomyocytes in combination with pulse-chase amino acid labelling and proteomics to analyse the effects of prolyl hydroxylation on protein degradation and synthesis. We identified 167 proteins that exhibit differences in degradation with inhibition of prolyl hydroxylation by dimethyloxalylglycine (DMOG); 164 were stabilized. Proteins involved in RNA splicing such as serine/arginine-rich splicing factor 2 (SRSF2) and splicing factor and proline- and glutamine-rich (SFPQ) were stabilized with DMOG. DMOG also decreased protein translation of cytoskeletal and sarcomeric proteins such as α-cardiac actin. We searched the mass spectrometry data for proline hydroxylation and identified 134 high confidence peptides mapping to 78 unique proteins. We identified SRSF2, SFPQ, α-cardiac actin, and cardiac titin as prolyl hydroxylated. We identified 29 prolyl hydroxylated proteins that showed a significant difference in either protein degradation or synthesis. Additionally, we performed next-generation RNA sequencing and showed that the observed decrease in protein synthesis was not due to changes in mRNA levels. Because RNA splicing factors were prolyl hydroxylated, we investigated splicing ± inhibition of prolyl hydroxylation and detected 369 alternative splicing events, with a preponderance of exon skipping.

Conclusions This study provides the first extensive characterization of the cardiac prolyl hydroxylome and demonstrates that inhibition of α-ketoglutarate hydroxylases alters protein stability, translation, and splicing.

Keywords Prolyl hydroxylation • Hypoxia • Proteomics • Protein degradation • Splicing

1. Introduction

Oxygen- and α-ketoglutarate-dependent enzymes are part of a superfamily of protein hydroxylases that catalyse the hydroxylation of amino acid residues such as prolines.[1–4] Because of the requirement for oxygen, prolyl hydroxylases can function as oxygen/hypoxia sensors; however, the K_m for oxygen varies among the family members.[5] Prolyl hydroxylase domain proteins (PHDs), also known as hypoxic inducible factors (HIF) prolyl 4 hydroxylases (H-P4H), hydroxylate prolines on HIF-1α which target it for degradation.[6–8] In addition to HIF-1α, the β_2-adrenergic receptor has been shown to undergo prolyl hydroxylation, which leads to its degradation, and hypoxia or inhibition of prolyl

* Corresponding author. Systems Biology Center, National Heart, Lung, and Blood Institute, National Institutes of Health, Building 10, Room 8N202, 10 Center Drive, Bethesda, MD 20892, USA. Tel: +1 301 496 5828; fax: +1 301 402 0190, E-mail: murphy1@nhlbi.nih.gov

hydroxylation leads to its stabilization.[9] As α-ketoglutarate is a substrate and succinate an end-product inhibitor, these metabolites can also regulate prolyl hydroxylase activity,[10,11] and a number of tumour cells have mutations in succinate dehydrogenase leading to an increase in succinate, inhibition of PHD proteins, and up-regulation of HIF-1α.[12] Thus, depending on the K_m of these enzymes for oxygen and α-ketoglutarate, they can be regulated by oxygen as well as by metabolism. Ribosomal prolyl hydroxylases [2-oxoglutarate and iron-dependent oxygenase domain containing 1 (OGFOD1) and Tpa1] have recently been described and shown to hydroxylate prolines in the ribosomal protein RPS23 leading to altered translation.[13–16]

In spite of the large and growing family of prolyl hydroxylases, only a small number of prolyl hydroxylated proteins have been identified.[9,13,17,18] This study provides the first large-scale proteomic characterization of the cardiac prolyl hydroxylome. Furthermore, it is clear that prolyl hydroxylation regulates cell functions that are independent of HIF. To better define the novel functional consequences of prolyl hydroxylation and to test the hypothesis that α-ketoglutarate-dependent hydroxylases broadly regulate protein stability, we performed a pulse-chase experiment with stable isotope-labelled amino acids using a cellular model of human induced pluripotent stem cell-derived cardiomyocytes (iPSC-CM).[19] It has been shown that the majority of newly synthesized proteins in non-dividing cell cultures use an extracellular, non-limiting, source of amino acids.[20,21]

To inhibit α-ketoglutarate-dependent hydroxylases, we used a cell-penetrating derivate of *N*-oxalylglycine (NOG), dimethyloxalylglycine (DMOG), which is an unreactive α-ketoglutarate analogue. DMOG is metabolized to NOG, which acts as a competitive inhibitor of α-ketoglutarate-dependent hydroxylases.[22–24] We found that inhibition of α-ketoglutarate-dependent hydroxylases increased the stability of a large number of proteins and reduced the rate of protein synthesis. Using next-generation RNA sequencing (RNA-seq), we demonstrated that the decrease in the rate of protein synthesis was not due to a change in the level of mRNA. Because the stability and/or translation of a number of ribosomal proteins and splicing factors were altered by inhibition of prolyl hydroxylation, we examined the RNA-seq data to identify differentially expressed splicing variants between control and hydroxylase inhibition. Interestingly, we found that inhibition of prolyl hydroxylases can alter exon skipping events. Taken together, the data in this study demonstrate that inhibition of prolyl hydroxylation alters protein stability, translation, and splicing in human cardiomyocytes. This study identifies a new role for prolyl hydroxylation in regulating RNA splicing.

2. Methods

2.1. Cardiac differentiation of iPSC and cardiomyocyte cell culture

iPSC were generated from human dermal fibroblasts by reprogramming as previously described.[25] Additional details are provided in the Supplementary material online, *Methods*.

2.2. Pulse-chase isotopic labelling with amino acids in iPSC-CM

iPSC-CM were equilibrated in light medium containing 10% dialysed foetal bovine serum for 3 days and underwent the Pierce SILAC protein quantification kit as described by the manufacturer. Further details are described in the Supplementary material online, *Methods*.

2.3. Mass spectrometry and data analysis

Protein identification by LC–MS/MS analysis of peptides was performed using an Orbitrap Fusion Tribid mass spectrometer (Thermo Fisher Scientific, San Jose, CA, USA) interfaced with an Ultimate 3000 Nano-HPLC apparatus (Thermo Fisher Scientific, San Jose, CA, USA). The mass spectrometry proteomics data have been deposited to the ProteomeXchange Consortium via the PRIDE[26] partner repository with the data set identifier PXD003621. Details are provided in the Supplementary material online, *Methods*.

2.4. Identification of prolyl hydroxylated peptides

iPSC-CM samples as described in Section 2.2 were searched using oxidation on proline as a variable (*Figure 4A*). In detail, the LC–MS data were searched against the Swiss-Prot database [taxonomy *Homo sapiens* (human)] using Mascot (Matrix Science, London, UK; version 2.5.1). Parameters for the search engine were precursor mass tolerance at 20 ppm, fragment ion mass tolerance at 0.8 Da, and trypsin enzyme with 2 miscleavages with methyl methanethiosulfonate of cysteine as fixed modification and deamidation of glutamine and asparagine, oxidation of methionine, and oxidation of proline as variable modifications. Proteome Discoverer software (version 1.4) was used and the data were filtered for high peptide confidence [false discovery rate (FDR) of $<1\%$]. From the peptide sequence annotation, the proteins undergoing prolyl hydroxylation were identified.

2.5. cDNA library preparation and RNA-seq analysis

The RNA samples underwent the TruSeq® stranded total RNA sample preparation according to the manufacturer's protocols. Details are provided in the Supplementary material online, *Methods*.

2.6. mRNA isolation, bioanalyser analysis, and quantitative RT-PCR analysis

mRNA isolation was performed using the RNeasy® mini kit (Qiagen, Valencia, CA, USA), and the protocol was followed as described by the manufacturer. Details are provided in the Supplementary material online, *Methods*.

2.7. Data analysis

Data were expressed as means ± SEM. Student's *t*-test (two-tailed, homodynamic variance) was used to compare between two groups and two-way ANOVA was used for multiple comparisons. For all tests, a probability value of ≤ 0.05 was considered as significant. Proteome Discoverer software (version 1.4) was used and data were filtered for high peptide confidence (FDR of $<1\%$). For label-free analysis, light and heavy peptides were quantified separately using an in-house software QUantification withOut Isotope Labelling (QUOIL).[27] Data were filtered for ≥ 2 peptides/protein target. For RNA-seq analysis, the normalized output count per million (CPM) values were compared by generalized linear model between conditions. The differentially expressed transcripts were defined as ≥ 4-fold changes with 1% FDR as described under RNA-seq analysis.

3. Results

3.1. Regulation of protein degradation

Prolyl hydroxylation has been shown to enhance degradation of several proteins, including HIF-1α and the β_2-adrenergic receptor. To evaluate if prolyl hydroxylation more widely alters the stability of proteins, we performed a non-biased, proteomic study to identify proteins that exhibit a change in turnover following addition of DMOG, an inhibitor of oxygen- and α-ketoglutarate-dependent hydroxylases. Because we

wanted to minimize changes in protein turnover that might be secondary to changes initiated by HIF, we examined changes that occurred with relatively short treatment times with DMOG. Human iPSC-CM were used as illustrated in *Figure 1A*. Cells were cultured in light medium and then switched to heavy medium and simultaneously treated with vehicle or DMOG. After switching to heavy medium, newly synthesized proteins will incorporate heavy amino acids, and the rate of decay of the light peptides provides a measure of protein

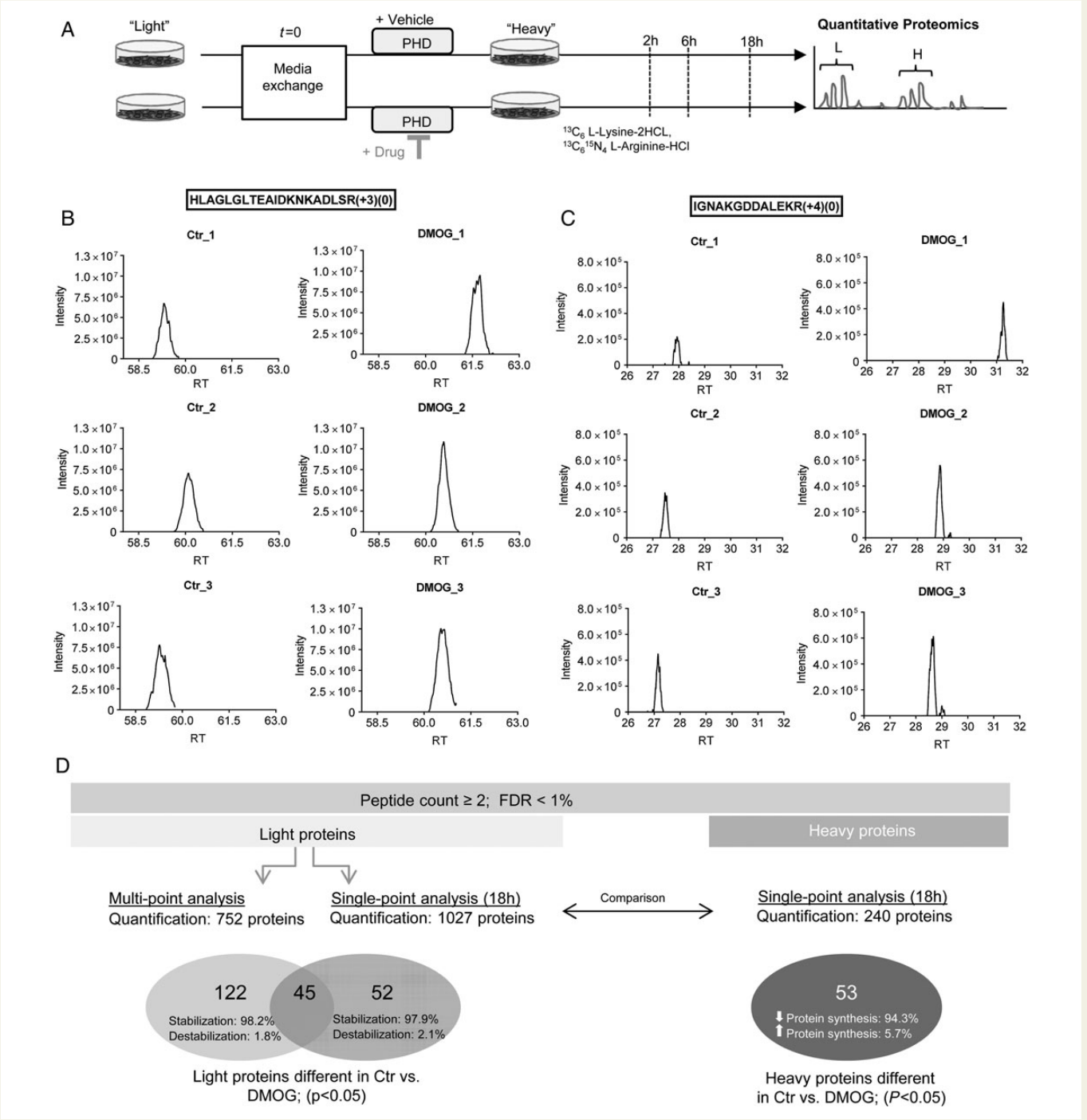

Figure 1 Analysis of pulse-chase labelled amino acids in human iPSC-derived cardiomyocytes by mass spectrometry. (*A*) Human iPSC-derived cardiomyocytes were analysed 23 days after initiation of differentiation. Cardiomyocytes were adapted to dialysed foetal bovine serum containing light medium for 3 days and then switched to heavy label ($^{13}C_6$ L-lysine-2HCl, $^{13}C_6^{15}N_4$ L-arginine-HCl). Cells were separated into two groups: vehicle and DMOG (1 mM). After 2, 6, and 18 h, groups were harvested and underwent tryptic digestion and mass spectrometry analysis. Representative ion chromatographs are shown for light peptides identified as significantly different (determined by QUOIL) between control and DMOG 18 h after switching to heavy media for the peptide HLAGLGLTEAIDKNKADLSR from Serpin H1 (*B*) and IGNAKGDDALEKR from Phosphoserine aminotransferase (*C*). Peaks are shown from three biological samples per group. (*D*) Summary of the proteomic analysis. See Supplementary material online, *Methods* for details.

degradation (Supplementary material online, *Figures S1A and S1B*). Heavy and light peptide groups were quantified separately with label-free analysis.[27] Representative ion chromatographs of light peptide areas at the 18 h time point are shown in *Figure 1B and C*. The reproducibility of the peptide quantitation is illustrated in Supplementary material online, *Figure S2*.

We used both a multi-point and a single-point approach to determine differences in protein degradation between control and DMOG as illustrated in *Figure 1D*. We found 752 proteins that were present in control and DMOG groups at all three times. We performed a first-order fit of the decay of light peptides on these 752 proteins and found 167 proteins that showed significant differences between control and DMOG ($P < 0.05$; Supplementary material online, *Excel Table S1*). A volcano plot shows light proteins that were significantly different between control and DMOG (*Figure 2A*). The vast majority of proteins with a significant difference had reduced degradation with DMOG treatment. Examples of the fitting are shown in *Figure 2B* for representative proteins. Using first-order decay analysis, we calculated protein half-life and found a median value of 22.7 h in control (*Figure 2C*) and 35.2 h in DMOG (*Figure 2D*).

To facilitate comparison with the heavy peptide data, we measured differences in light peptide levels at 18 h of treatment, and as shown in the volcano plot (Supplementary material online, *Figure S1C*), we identified many peptides that showed a significant difference in degradation. Supplementary material online, *Excel Table S2* shows 97 proteins that were significantly different between the groups ($P < 0.05$, peptides ≥ 2). Consistent with the fitting data in *Figure 2* and Supplementary material online, *Excel Table S1*, the 18 h data showed that all but two proteins were stabilized by addition of DMOG. Thus, as summarized in *Figure 1D*, in the multi-point analysis, 167 proteins were identified as being significantly different between control and DMOG and 98.2% of those showed an increase in protein stability. In the single-point analysis, 97 proteins were significantly different, and 97.9% of those showed an increase in protein stability.

We performed PANTHER (Protein ANalysis THrough Evolutionary Relationships) protein class analysis on proteins with reduced degradation and found changes in proteins involved in nucleic acid binding (13.6%) and cytoskeletal function (12.6%; *Figure 3A*). The nucleic acid binding protein group was enriched for RNA-binding proteins involved in mRNA processes, such as alternative splicing (*Figure 3B*). We also

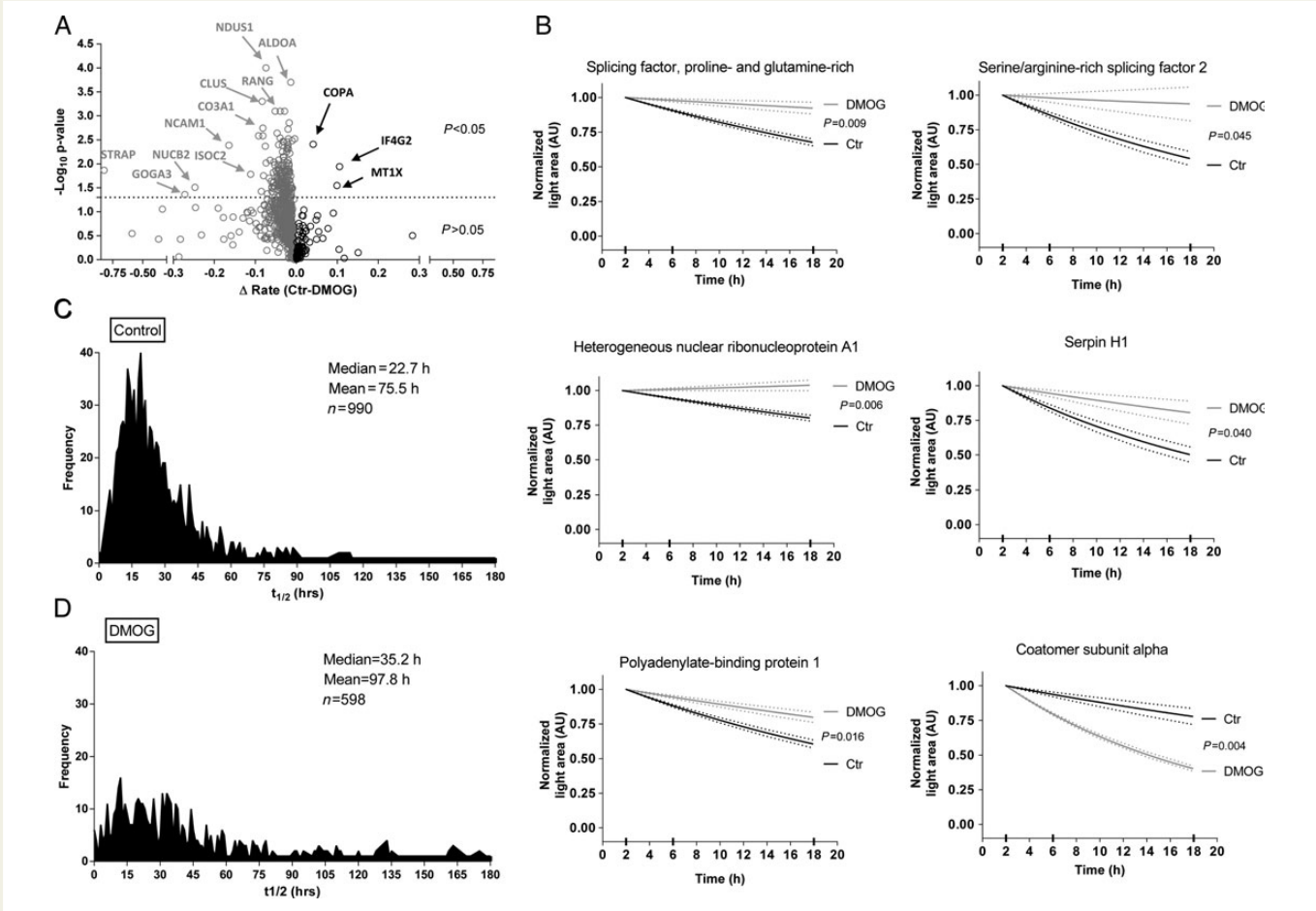

Figure 2 Quantitative assessment of light proteins. (*A*) Volcano plot analysis shows the distribution of light proteins between control and DMOG. First-order kinetic slopes were calculated from three time points. Two-way ANOVA was used for calculating the *P*-values from the fit of first-order equations. Interesting targets are labelled and highlighted by arrows. Proteins stabilized by DMOG are on the left side and those destabilized are on the right of the origin. Y-axis shows the negative $\log_{10}$ *P*-value and the X-axis shows the differences in rate (control − DMOG). (*B*) Representative fits for selected proteins. The dotted lines show the measure of error. Distribution of protein half-lives under control (*C*) or DMOG (*D*) obtained by the first-order equations to multi-point data (2, 6, and 18 h). Light peptide areas are shown normalized to the 2 h time point for both groups.

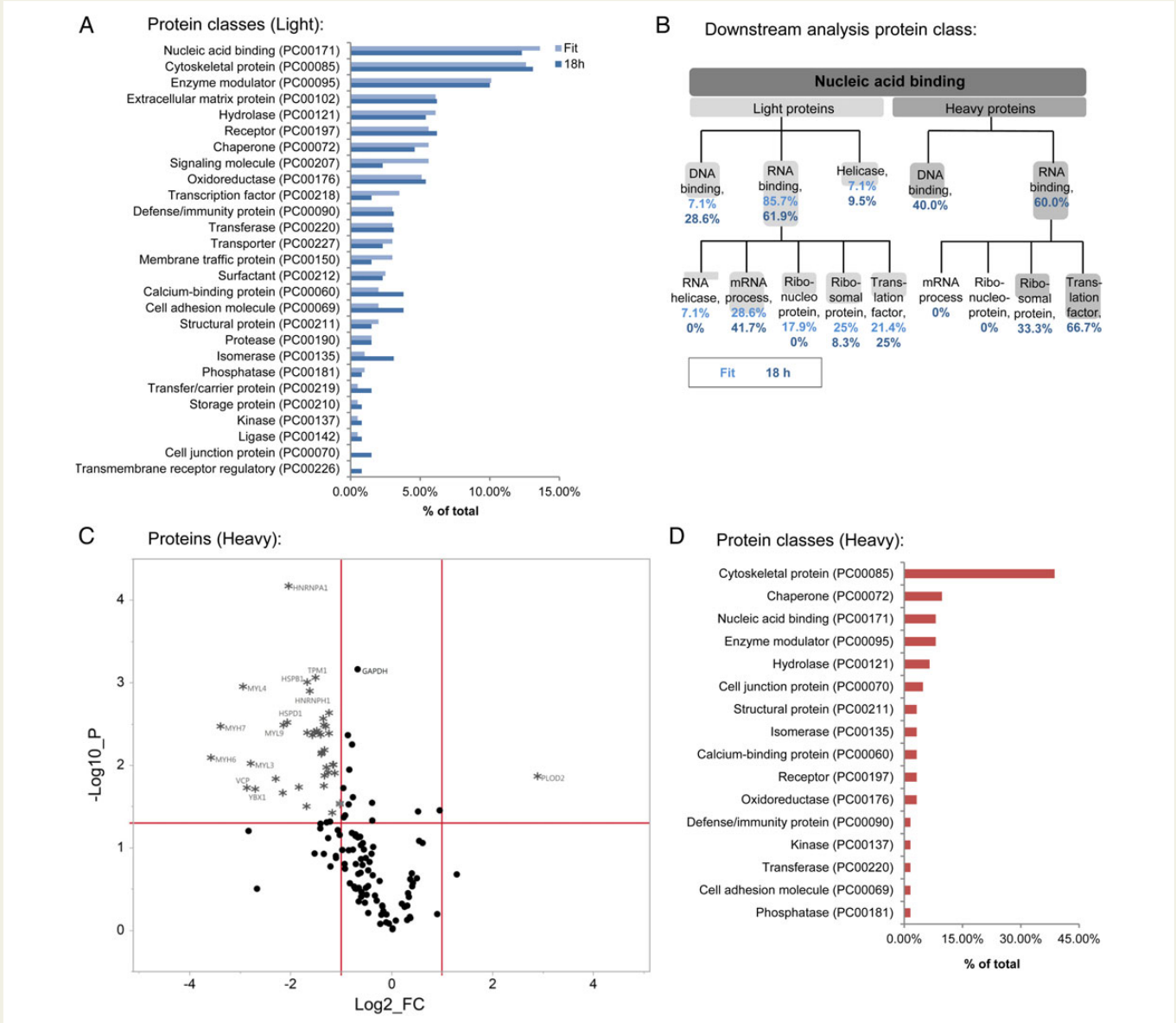

Figure 3 Analysis for light and heavy proteins. (*A*) Using the online tool PANTHER classification system, protein class analysis was performed for light proteins that were significantly stabilized in the presence of DMOG as analysed by the multiple-point method or the single-point method (18 h). Percentage of total number of identified protein classes are shown. (*B*) Further characterization shows that the nucleic acid binding proteins were enriched for RNA-binding targets. (*C*) A volcano plot depicts the heavy proteins measured with the single-point method after 18 h. The horizontal line represents $P = 0.05$, the vertical lines represent the threshold for the $\log_2$ fold change ($\log_2$FC). (*D*) Using PANTHER, protein class analysis was performed for heavy protein targets that showed a significant reduction in protein synthesis with DMOG (18 h, single-point method). Synthesis of cytoskeletal proteins was strongly affected by DMOG.

performed PANTHER pathway analysis (Supplementary material online, *Figures S3*) and used IPA® software to examine differences in network interaction in proteins that showed a difference in stability following DMOG. Interactions in networks involving cell survival (Supplementary material online, *Figure S4*) and transcriptional regulation and mRNA processing (Supplementary material online, *Figure S5*) were observed.

3.2. Differences in the rate of protein synthesis with DMOG

We further determined if inhibition of prolyl hydroxylation alters protein translation. Label-free analysis was performed following DMOG to determine the rate of incorporation of heavy peptides, which reflects the rate of protein synthesis. A total of 53 proteins exhibited a significant difference between control and DMOG ($P < 0.05$; Supplementary material online, *Table S1*). A volcano plot for heavy proteins and peptides is shown in *Figure 3C* and Supplementary material online, *Figure S1D*, respectively. Interestingly, DMOG primarily decreased protein synthesis relative to control. The 53 proteins, which show a significant change in translation, are highly enriched for contractile and cytoskeletal proteins. Furthermore, protein synthesis of heterogeneous nuclear ribonucleoproteins (which are involved in RNA processing), heat shock proteins, histones, and elongation factors were decreased. Pathway analysis (Supplementary material online, *Figure S3C*) shows

enrichment of pathways involving cytoskeletal regulation by Rho GTPase. Protein class analysis shows that DMOG causes changes in translation of cytoskeletal proteins, chaperones, and nucleic acid binding proteins (*Figure 3D*). RNA-binding proteins accounted for 60% of the nucleic acid binding group, most of them were translation factors (66.7%; *Figure 3B*).

3.3. Identification of the cardiac prolyl hydroxalome

Next, we identified novel sites of prolyl hydroxylation in the samples obtained from the pulse-chase amino acid labelling study (*Figure 4A*). Given the large number of proteins that catalyse proline hydroxylation, we hypothesized that there are likely to be additional uncharacterized proteins with proline hydroxylation. We filtered out collagen and peptides that were only present in one sample, yielding 95 prolyl hydroxylated light peptides and 39 prolyl hydroxylated heavy peptides, which mapped to 78 proteins (Supplementary material online, *Excel Table S3*). Representative spectra are shown in Supplementary material online, *Figure S6*. We identified several isoforms of protein disulfide isomerase (PDIA1, PDIA3, PDIA4, PDIA6), which is a multifunctional protein that is also a subunit of prolyl 4 hydroxylase. We observed prolyl hydroxylation of several splicing factors and RNA-binding proteins (*Table 1*). Cardiac actin (proline 72) was also found to be prolyl hydroxylated. Non-muscle actin was recently reported to undergo prolyl hydroxylation at prolines 307 and 322.[17] Gene ontology analysis of prolyl hydroxylated proteins showed enrichment in RNA binding, poly(A) RNA binding, and protein disulfide isomerase activity (*Figure 4B*). PANTHER protein class analysis showed that prolyl hydroxylated proteins were mainly cytoskeletal and nucleic acid binding proteins (*Figure 4C*), and PANTHER pathway analysis identified prolyl hydroxylated proteins to be involved in cytoskeletal regulation (Supplementary material online, *Figure S7*).

As shown in *Table 1* in detail, 29 of the 78 prolyl hydroxylated proteins exhibited a change in protein degradation or translation. The overlap is illustrated in *Figure 4D*. These data suggest that there are many additional, unidentified roles for prolyl hydroxylation.

To analyse the effect of DMOG on prolyl hydroxylation, we investigated light and heavy proteins separately. For the light peptides, which are present in pre-existing proteins, the level of proline hydroxylation

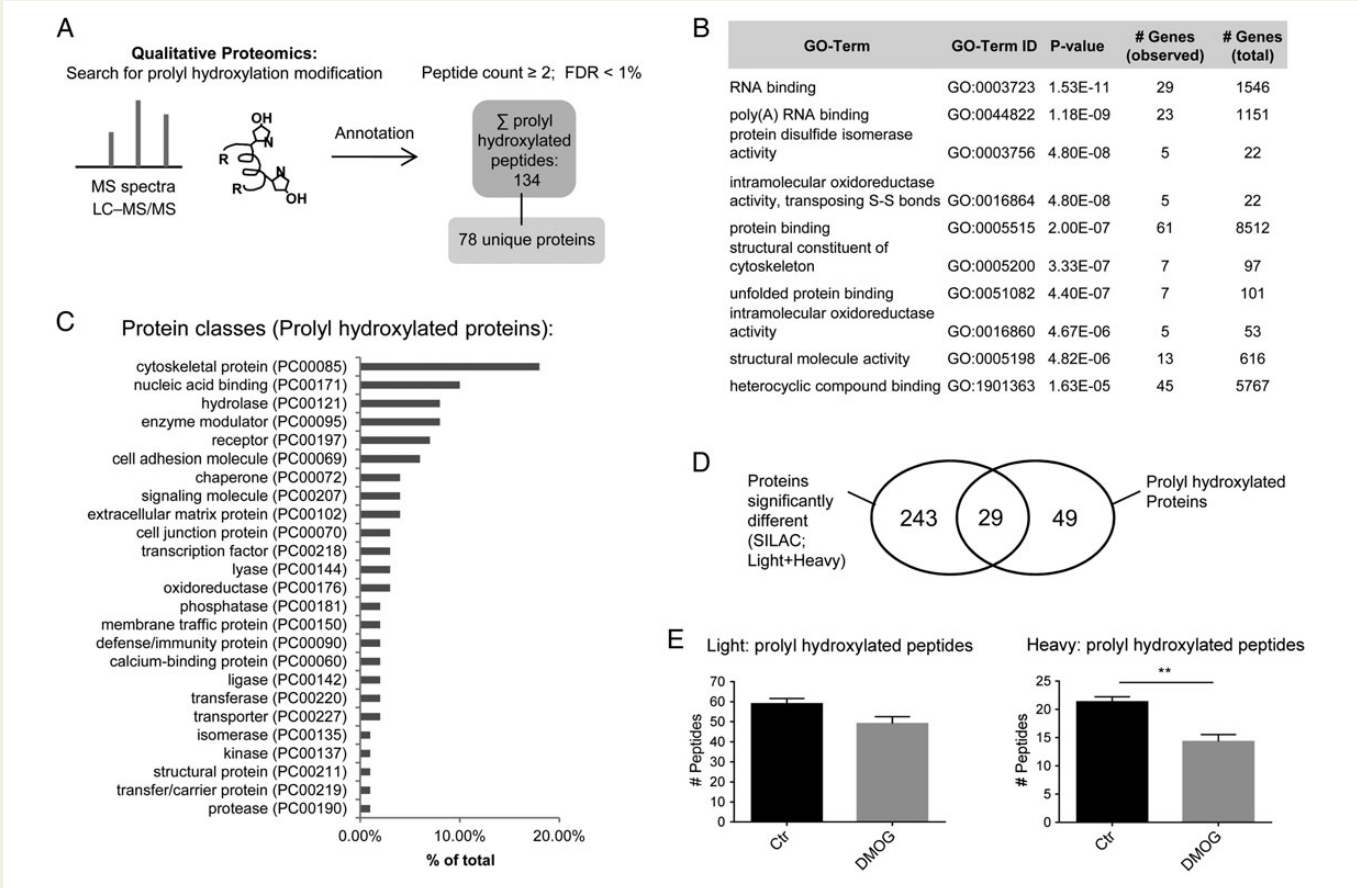

Figure 4 Identification of prolyl hydroxylated peptides using mass spectrometry analysis of the pulse-chase labelled amino acids in human iPSC-CM. (*A*) The mass spectrometric data from the Orbitrap Fusion system was searched for proline oxidation in control ($n = 3$) and DMOG ($n = 3$) samples. Proteome Discoverer software (version 1.4) was used to filter the data for high peptide confidence (FDR of <1%) to identify prolyl oxidated peptides and for annotation to the respective proteins. Prolyl hydroxylated peptides were identified in at least two out of six samples. (*B*) Genomatrix Genome Analyser software was used to identify enriched gene ontology (GO) terms for the prolyl hydroxylated proteins. Listed here are the top 10. (*C*) Protein class analysis was performed for prolyl hydroxylated proteins identified in mass spectrometric analysis with PANTHER. Protein classes are shown as percentage of total number of identified protein classes. (*D*) Schematic illustration for overlap between prolyl hydroxylated proteins and proteins with a change in degradation/synthesis. (*E*) Effect of DMOG on the number of light vs. heavy prolyl hydroxylated peptides. Data are shown ± SEM. $^{**}P < 0.01$ vs. control (Student's *t*-test).

Table I Prolyl hydroxylated proteins

#	Protein name and accession number	Sequence	Protein stability	Protein synthesis
1	Actin, alpha cardiac muscle 1, P68032	GILTLKY***p***IEHGIITNWDDMEKIWHHTFYNELR KYSVWIGGSILASLSTFQqMWISKQEYDEAG***p***SIVHRK RGILTLKY***p***IEHGIITNWDDMEKIWHHTFYNELR VAPEEHPTLLTEAPLN***p***KANREk YSVWIGGSILASLSTFQQMWISKQEYDEAG***p***SIVHRK	–	↓
2	Actin, cytoplasmic 1, P60709	GILTLKY***p***IEHGIVTNWDDMEKIWHHTFYNELR LcYVALDFEqEMATAASSSSLEKSYEL***p***DGQVITIGNER rGILTLKY***p***IEHGIVTnWDDMEKIWHHTFYnELR rGILTLkY***p***IEHGIVTNWDDMEkIWHHTFYNELr RGILTLKY***p***IEHGIVTNWDDMEKIWHHTFYNELR VAPEEHPVLLTEAPLN***p***KANR Y***p***IEHGIVTNWDDMEKIWHHTFYNELR	–	↓
3	Actin, gamma-enteric smooth muscle, P63267	GILTLKY***p***IEHGIITNWDDMEKIWHHSFYNELR IIAPPERKYSVWIGGSILASLSTFQQmWISK***p***EYDEAGPSIVHR KYSVWIGGSILASLSTFQQmWISK***p***EYDEAGPSIVHR KYSVWIGGSILASLSTFQQmWISk***p***EYDEAGPSIVHrk	–	↓
4	Desmoplakin, P15924	IGLVrPGTALELLEAQAATGFIVDPVSNLRL***p***VEEAYKr	↑	–
5	**Elongation factor 1-alpha 1, P68104**	kDGNASGTTLLEALDcILP***p***TrPTDkPLRLPLQDVYk kDGNASGTTLLEALDcILPPTrPTDKPLRL***p***LqDVYk VETGVLK***p***GMVVTFAPVNVTTEVK	–	↓
6	Fibronectin, P02751	cD***p***VDQcqDSETGTFYQIGDSWEK FTNIG***p***DTmrVTWA***p***PPSIDLTNFLVR GRWKcD***p***VDQcqDSETGTFYQIGDSWEk GRWKcD***p***VDQcQDSETGTFYQIGDSWEk TqGNKQMLcTcLGNGVScQETAVTQTYGGNSnGE***p***cVLPFTYnGR TqGnKQMLcTcLGNGVScQETAVTQTYGGnSnGE***p***cVLPFTYnGR TqGNKQMLcTcLGNGVScQETAVTQTYGGnSnGEPcVL***p***FTYnGR TqGNKQMLcTcLGNGVScQETAVTQTYGGNSNGE***p***cVLPFTYnGR VGDTYER***p***KDSMIWDcTcIGAGr	↑	–
7	**Heterogeneous nuclear ribonucleoprotein A1, P09651**	SHFEQWGTLTDcVVMrD***p***NTKR GFGFVTYATVEEVDAAmnAR***p***HKVDGr	↑	↓
8	Prolyl 4-hydroxylase subunit alpha-1, P13674	FHDIISDAEIEIVkDLAK***p***R	↑	–
9	Pyruvate kinase PKM, P14618	AEGSDVANAVLDGADcIMLSGETAKGDY***p***LEAVR KGDVVIVLTGWR***p***GSGFTNTMR TATESFASDPILYR***p***VAVALDTKGPEIr	↑	–
10	**Serine/arginine-rich splicing factor 2, Q01130**	SYGr***pp***PDVEGMTSLKVDNLTYR	↑	–
11	Serpin H1, P50454	KPAAAAA***p***GTAEKLSPK SALQSINEWAAQTTDGkL***p***EVTKDVER	↑	–
12	Tenascin, P24821	GLcVDGQcVcEDGFTGPDcAELSc***p***nDcHGqGr WQPAIATVDSYVISYTGEKV***p***EITR	↑	–
13	Tubulin beta-3 chain, Q13509	LHFFMPGFA***p***LTAr LHFFMPGFA***p***LTAR LHFFmPGFA***p***LTAR	↑	↓
14	60 kDa heat shock protein, mitochondrial, P10809	TALLDAAGVASLLTTAEVVVTEI***p***KEEKDPGmGAMGGMGGGMGGGMF	–	↓
15	Cofilin-1, P23528	ML***p***DKDcR NIILEEGKEILVGDVGqTVDD***p***YATFVK	↑	–
16	**Elongation factor 2, P13639**	WLPAGDALLQMITIHLPS***p***VTAQKYR	↑	↓
17	Endoplasmin, P14625	GYEVIYLTEPVDEYcIQAL***p***EFDGKR TETVEEPMEEEEAAKEEKEESDDEAAVEEEEEEKK***p***K	↑	–
18	Heat shock protein beta-1, P04792	LPEEWSqWLGGSSWPGYVRPLPPAAIES***p***AVAAPAYSR YTLPPGVD***p***TqVSSSLSPEGTLTVEAPMPK	↑	↓
19	Myosin-6, P13533	A***p***GVMDNPLVMHQLR	–	↓
20	Palladin, Q8WX93	SAPAMQSSGSFNYAR***p***K	–	↓
21	PDZ and LIM domain protein 1, O00151	VITNQYNn***p***AGLYSSENISNFNNALESK	↑	–

Continued

Table 1 *Continued*

#	Protein name and accession number	Sequence	Protein stability	Protein synthesis
22	Protein disulfide isomerase A3, P30101	ISDTGSAGLMLVEFFA***p***WcGHcKR ISDTGSAGLmLVEFFA***p***WcGHcKR	↑	–
23	**Protein disulfide isomerase A4, P13667**	ENFDEVVNDADIILVEFYA***p***WcGHcKK KDVLIEFYA***p***WcGHcK	↑	–
24	Protein disulfide isomerase A6, Q15084	EVIQSDSLWLVEFYA***p***WcGHcQR	↑	–
25	Protein disulfide isomerase OS, P07237	KNVFVEFYA***p***WcGHcK NFEDVAFDEKKNVFVEFYA***p***WcGHcK NVFVEFYA***p***WcGHcK YLLVEFYA***p***WcGHcK	↑	–
26	**Splicing factor, proline- and glutamine-rich, P23246**	NLS***p***YVSnELLEEAFSQFGPIER	↑	–
27	T-complex protein 1 subunit delta, P50991	AFADAMEVI***p***STLAEnAGLNPISTVTELR AFADAMEVI***p***STLAEnAGLNPISTVTELR AFADAMEVI***p***STLAEnAGLNPISTVTELR	↑	–
28	**Transitional endoplasmic reticulum ATPase, P55072**	GFGSFRFPSGNqGGAG***p***SqGSGGGTGGSVYTEDNDDDLYG GFGSFRFPSGNQGGAG***p***SqGSGGGTGGSVYTEDNDDDLYG	↑	↓
29	**Tubulin beta-4B chain, P04350**	AVLVDLE***p***GTMDSVR	–	↓

Prolyl hydroxylated peptides were also identified as showing a difference in protein stability/synthesis in the pulse-chase amino acid labeling quantification. Proteins were identified by LC–MS/MS and accession numbers and protein IDs are from the Swiss-Prot/Uniprot databases. The hydroxylated proline residue is in bold and italicized. Peptides were filtered to 1% FDR using the Percolator algorithm in Thermo Proteome Discoverer software. Other post-translational modifications are represented by lower case letters: m stands for oxidation of methionine, c stands for methyl methanethiosulfonate of cysteine, n stands for deamidation of asparagine, q stands for deamidation of glutamine. Further details for the Ion Score (Mascot Score) and the posterior error probability (characterizes the probability that the observed peptide spectrum matched (PSM) is incorrect) can be found in Supplementary material online, *Excel Table S3*. RNA-binding proteins and splicing factors are in bold.

was similar between control and DMOG. This would be consistent with the lack of an enzyme to remove proline hydroxylation. When we analysed the heavy label, which is present in newly synthesized proteins, we found significantly less prolyl hydroxylation with DMOG vs. control (*Figure 4E*).

3.4. Changes in the cardiomyocyte transcriptome following hydroxylase inhibition

To determine if the changes in protein synthesis with DMOG observed in *Figure 3C* were due to alterations in mRNA, we analysed changes in the mRNA expression profiles in control and 18 h DMOG-treated cardiomyocytes. Principle component analysis (*Figure 5A*) and heat map clustering (*Figure 5B*) showed a clear separation between control and DMOG. We identified 352 transcripts (Supplementary material online, *Excel Table S4*) with at least a four-fold difference between control and DMOG (FDR $<1\%$, complete data set is available online: GSE71560 accession number). A volcano plot of the 352 transcripts shows an equal distribution between mRNAs with an increase and decrease in expression (*Figure 5C*). In contrast to the mRNA data, the proteomics data showed a preponderance of proteins with a decrease in protein synthesis after DMOG treatment (Supplementary material online, *Table S1*). When we compared the changes of mRNA vs. the changes in protein synthesis, we found a poor correlation (*Figure 5D*).

3.5. Hydroxylase inhibition promotes alternative splicing

We found proline hydroxylation of several RNA splicing factors and RNA-binding proteins (*Table 1* and Supplementary material online, *Excel Table S3*), and this, along with the finding that DMOG altered synthesis and stabilization of RNA-binding proteins, led us to investigate alternative splice variants. Using mixture of isoforms software, we detected 369 alternative splicing events that were different between control and DMOG, with a preponderance of exon skipping (Supplementary material online, *Excel Table S5*). The details of the different splicing events are shown in Supplementary material online, *Table S2* (complete data set is available online: GSE71560 accession number). As shown in *Figure 6A*, using IPA® software, these alternatively spliced genes are enriched in leucine and isoleucine degradation as well as the NAD salvage pathway. *Figures 6B and C* show sashimi plots and the frequency distributions for mitochondrial branched-chain-amino-acid aminotransferase (BCAT2), an enzyme involved in leucine and isoleucine degradation, and cytosolic purine 5′-nucleotidase II (NT5C2), which is involved in the NAD salvage pathway. With DMOG, BCAT2 exhibited reduced exon skipping and NT5C2 exhibited increased exon skipping (*Figure 6D*). Using Homer analysis, we found a purine-rich motif enriched in differentially spliced exons compared with a randomly shuffled sequence background (*Figure 6E*). Since serine/arginine (SR)-rich splicing factors are known to bind to purine-rich motifs,[28,29] our finding implies that DMOG-dependent alternative splicing might be mediated by SR family splicing factors, which we observed to be prolyl hydroxylated and whose protein stability was found to be altered with DMOG. We further scanned 260 SR-rich splicing factor 2 (SRSF2) exon skipping event sequences and identified common AGG-boxes, indicating that SRSF2 might be involved in mediating the observed differences. Taken together, these results support the notion that inhibition of oxygen- and α-ketoglutarate-dependent hydroxylases can lead to alteration in splicing.

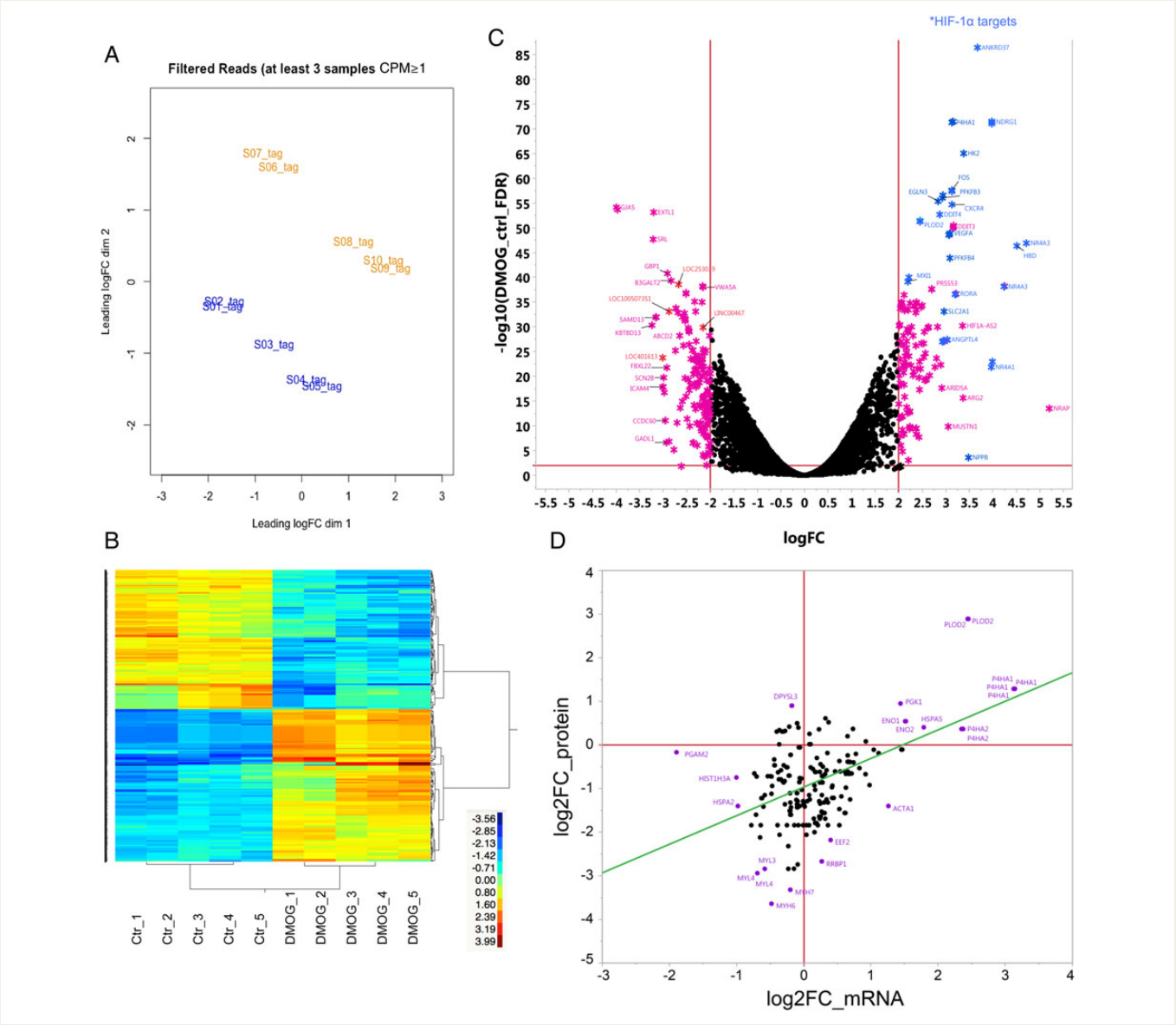

Figure 5 Comparison of the cardiac transcriptome and protein translation. iPSC-derived cardiomyocytes were analysed 18 h after vehicle (control) or DMOG. (*A*) Principle component analysis of control ($n = 5$) and DMOG ($n = 5$) mRNA samples from RNA-seq. Blue label indicates the control group and orange label indicates DMOG. Clustering analysis showed sample grouping within the respective treatment. (*B*) Heatmap gene clustering analysis of control and DMOG samples (after 18 h). The expression for each gene is shown in rows, and samples are clustered in columns. The expression levels of each gene across the samples are shown as $\log_2$CPM (counts). The scaled expression values are colour-coded according to the legend. The dendrogram depicting hierarchical clustering is based on the expression of significantly different genes. (*C*) Volcano plot of mRNA-sequencing data. The horizontal line represents the false-positive control (FDR) at 1%, the vertical lines represent the threshold for the $\log_2$ fold change ($\log_2$FC). The X-axis depicts the $\log_2$ difference in estimated relative expression values. Vertical lines represent the threshold for the $\log_2$ fold change. The DMOG transcripts that are up-regulated (right) or down-regulated (left) greater than four-fold are marked as *. Previously described HIF-1α target genes are highlighted in blue. (*D*) Correlation between differences in proteins (heavy) and mRNA synthesis ± DMOG.

4. Discussion

This study applied a multi-pronged approach to investigate biological effects of oxygen- and α-ketoglutarate-dependent hydroxylases in human cardiomyocytes. Excluding collagen, we identified a large number of novel proteins exhibiting proline hydroxylation. We found 134 high confidence peptides mapping to 78 unique proteins. Of particular interest, 37% of prolyl hydroxylated proteins exhibited reduced rates of degradation and/or reduced rates of translation with inhibition of prolyl hydroxylation. There are two general possibilities for the modest overlap between proline hydroxylation and alterations in protein stability/synthesis. It is likely that prolyl hydroxylation regulates additional processes. For example, prolyl hydroxylation of actin has been shown to reduce actin polymerization,[17] and prolyl hydroxylation of the human homologue of the *Caenorhabditis elegans* biological clock protein CLK-2 (HCLK2) enhances its binding to and activation of ataxia telangiectasia and Rad3-related kinase (ATR/CHK).[30] Alternatively, large-scale proteomic approaches do not capture all of the modified

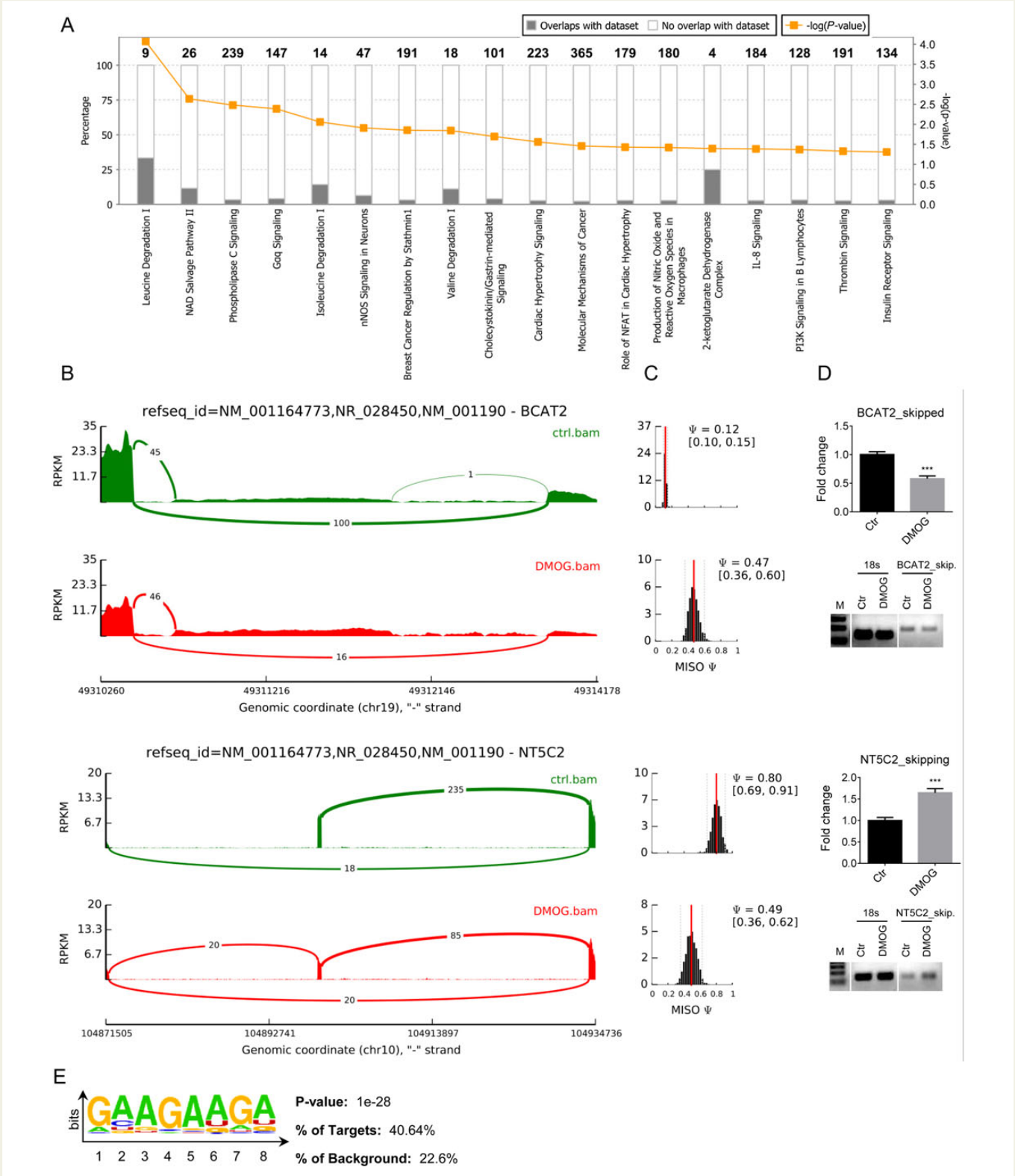

Figure 6 RNA-seq data. (*A*) Pathway analysis for splice variants by the Ingenuity Pathway Analysis (IPA®) showed differences in exon skipping between control and DMOG ($n = 5$ per group). The *P*-value was calculated by IPA® based on Fisher's exact test. The percentage characterizes the number of identified genes associated with that pathway. (*B*) Sashimi plot and frequency analysis for two targets: BCAT2, involved in the branched-chain-amino-acid degradation pathway, and NT5C2, in the NAD salvage pathway. (*C*) The width of the interval corresponds to the confidence in the estimate of the **Ψ** value. (*D*) Exon skipping changes with DMOG for BCAT2 and NT5C2 were verified using qRT-PCR and visualized on an agarose gel. 18s RNA was used as a control. (*E*) HOMER analysis identified enriched binding motifs within splicing region sequences comparing to the shuffled background sequences. Purine-rich 7-mer 'GAAGAAG' was identified in the splicing-exon regions. Data are shown ± SEM. ***$P < 0.001$ vs. control (Student's *t*-test).

proteins. It is possible that there are additional unidentified prolyl hydroxylated proteins and additional proteins with altered protein stability.

We analysed the prolyl hydroxylation data to determine if prolyl hydroxylation is altered by DMOG. As there is no known enzyme to remove prolyl hydroxylation, we were not surprised that there was no difference in the level of prolyl hydroxylation in the light peptides, which label the proteins existing prior to addition of DMOG. However, as the heavy label is present in newly synthesized peptides, we expected there to be significantly less prolyl hydroxylation in the DMOG vs. the control heavy label group, which was indeed the case (*Figure 4E*). These data are consistent with the lack of an enzyme to globally remove prolyl hydroxylation (we cannot rule out some selectively targeted removal enzymes).

Some recent papers have used proteomic approaches to enrich for prolyl hydroxylated proteins.[17,18,31] Arsenault *et al.* used a Von Hippel–Lindau (VHL) scaffold protein to bind and capture prolyl hydroxylation targets and identified five novel targets: FK506-binding protein 10, myosin heavy chain 10, hexokinase 2, pyruvate kinase, and C-1 tetrahydrofolate synthase. We did not identify these targets in our screen. Reasons for the lack of overlap include differences in cell type and the approach used for enriching for prolyl hydroxylation. Their approach would select for proteins that bind VHL and this is likely to be a subset of prolyl hydroxylated proteins. In another study, Luo *et al.* used an antibody against proline hydroxylation for enrichment in HeLa cells and reported one new target: non-muscle actin.[17] We identified a related protein, cardiac actin in our screen. Ratcliffe *et al.* applied a proteomics-based technique to identify substrates of asparaginyl hydroxylase factor inhibiting HIF (FIH). They used DMOG as a substrate trapping agent (it stabilizes the interaction) along with SILAC in U2OS cells to identify preferential DMOG-stabilized interactions with FIH and identified 13 new FIH-dependent hydroxylation sites.[31]

One of the best characterized effects of prolyl hydroxylation is targeting proteins for degradation. We hypothesized that there are many proteins in addition to HIF-1α and β-adrenergic receptor that are targeted for degradation by prolyl hydroxylation. This study is the first to perform a large-scale characterization of changes in the rate of protein degradation that are dependent on α-ketoglutarate-dependent hydroxylase activity in human cardiomyocytes. We found that DMOG promoted a decrease in protein degradation. These stabilized proteins are potential candidates for hypoxic signalling in the heart, and consistent with this concept, these proteins are involved in angiogenesis along with actin cytoskeleton regulation and RNA processing. Furthermore, our study provides important information on protein half-lives in human iPSC-CM. Alterations in protein degradation can have important physiological consequences, and only a handful of studies have comprehensively measured cardiac protein turnover rate,[32] and to our knowledge there are none in iPSC-CM, which are increasingly used as a model to study cardiac physiology and disease.[33]

We measured changes in protein synthesis following DMOG treatment and observed that inhibition of prolyl hydroxylation for 18 h results in inhibition of protein translation. It is noteworthy that hypoxia, which can regulate prolyl hydroxylation, has been shown to selectively reduce protein synthesis.[34] Furthermore, this decrease in protein synthesis following DMOG occurred in the absence of a change in mRNA levels, suggesting that inhibition of protein hydroxylation leads to a decrease in the rate of translation. A change in protein synthesis in the absence of a change in mRNA has been previously reported in hibernating animals.[34] Inhibition of OGFOD1, a newly described hydroxylase, has been reported to lead to a decrease in translation and stress granule formation.[13,35] Supplementary material online, *Table S1* shows that affected targets included tubulins, actin, and myosin. It is known that actin filaments in association with myosin are responsible for cellular movements. We saw decreased protein synthesis in cardiac-specific sarcomeric proteins such as myosin-6 and cardiac actin, which could affect contractility. It has been shown that cardiac contractility decreases in perfused rat hearts under hypoxia and cardiac hibernation.[36,37]

We observed that DMOG altered the rate of protein degradation and synthesis of a large number of RNA-binding and -regulatory proteins. Inhibition of hydroxylases increased the stability of SRSF2, splicing factor proline/glutamine-rich (SFPQ), and heterogeneous nuclear ribonucleoprotein A1. We also identified novel sites of prolyl hydroxylation on these proteins. Because of these findings, we hypothesized that DMOG might cause alterations in mRNA splicing. We further identified a significant difference in the rate of degradation of serine–threonine kinase receptor-associated protein in the presence of DMOG in comparison to control. Interestingly, this protein ('unrip') has been shown to bind to the macromolecular complex containing survival of motor neurons, which is involved in mediating the assembly of spliceosomal small nuclear ribonucleoproteins.[38,39]

We detected 369 alternative splicing events that differed between control and DMOG, with a preponderance of exon skipping. These data are consistent with studies reporting that hypoxia (which inhibits many prolyl hydroxylases) is associated with altered rates of protein synthesis, altered miRNAs, and altered splicing.[34,40,41] Alternative splicing has also been shown to occur in heart failure.[42] These findings are of interest given recent studies identifying novel prolyl hydroxylases that target ribosomal proteins that alter rates of translation and RNA processing.[2,13,14,35,43] We verified proteins such as BCAT2 and NT5C2 as being affected in exon skipping following DMOG treatment. The functional consequences of these modified splicing events will need to be investigated in future research.

DMOG in the millimolar range has been used by numerous groups to study the consequences of inhibition of α-ketoglutarate-dependent hydroxylases.[31,44–47] It has been shown that protein stabilization of HIF was not reproducibly seen with concentrations below 1 mM.[46] Additionally, previous studies showed that addition of 1 mM DMOG in cell culture medium for 7 days was not cytotoxic,[45,46,48] although a recent study reported that DMOG can acutely reduce oxygen consumption in HCT116 cells.[49] To assure complete inhibition of proline hydroxylation, 1 mM DMOG was used. Additionally, although DMOG is used in many studies as an inhibitor of HIF-PHDs, it inhibits a broad range of α-ketoglutarate-dependent oxygenases. Thus, examining the effect of DMOG provides an integrated picture of the effects of systematic inhibition of the α-ketoglutarate-dependent oxygenases in cardiac cells. It will be useful in future studies to tease out the precise α-ketoglutarate-dependent oxygenases responsible for the different effects of DMOG (alterations in splicing vs. translation vs. protein degradation).

In summary, this study provides the first extensive characterization of the prolyl hydroxylome, identifying over 100 sites of prolyl hydroxylation. Consistent with a regulatory role for many of these sites, we find that the rate of degradation and/or protein synthesis is altered for ~37% of these proteins (*Table 1*). Taken together, this study shows that inhibition of α-ketoglutarate-dependent hydroxylases results in alteration of protein synthesis and degradation and affects alternative splicing, which allows the cardiac cell to rapidly adjust to new conditions, such as hypoxia.

Supplementary material

Supplementary material is available at *Cardiovascular Research* online.

Acknowledgements

We thank Kim Woodhouse for excellent training with the bioanalyser. We thank Pablo Sandoval Concha for advice in the multi-point fitting analysis.

Conflict of interest: none declared.

Funding

This work was supported by the NIH-NHLBI Intramural Program.

References

1. Rose NR, McDonough MA, King ON, Kawamura A, Schofield CJ. Inhibition of 2-oxoglutarate dependent oxygenases. *Chem Soc Rev* 2011;**40**:4364–4397.
2. Markolovic S, Wilkins SE, Schofield CJ. Protein hydroxylation catalyzed by 2-oxoglutarate-dependent oxygenases. *J Biol Chem* 2015;**290**:20712–20722.
3. Gorres KL, Raines RT. Prolyl 4-hydroxylase. *Crit Rev Biochem Mol Biol* 2010;**45**:106–124.
4. Lando D, Peet DJ, Whelan DA, Gorman JJ, Whitelaw ML. Asparagine hydroxylation of the HIF transactivation domain a hypoxic switch. *Science* 2002;**295**:858–861.
5. Schofield CJ, Ratcliffe P. Oxygen sensing by HIF hydroxylases. *Nat Rev Mol Cell Biol* 2004;**5**:343–354.
6. Ivan M, Kondo K, Yang H, Kim W, Valiando J, Ohh M, Salic A, Asara JM, Lane WS, Kaelin WG Jr. HIFalpha targeted for VHL-mediated destruction by proline hydroxylation: implications for O_2 sensing. *Science* 2001;**292**:464–468.
7. Jaakkola P, Mole DR, Tian YM, Wilson MI, Gielbert J, Gaskell SJ, von Kriegsheim A, Hebestreit HF, Mukherji M, Schofield CJ, Maxwell PH, Pugh CW, Ratcliffe PJ. Targeting of HIF-alpha to the von Hippel-Lindau ubiquitylation complex by O_2-regulated prolyl hydroxylation. *Science* 2001;**292**:468–472.
8. Epstein AC, Gleadle JM, McNeill LA, Hewitson KS, O'Rourke J, Mole DR, Mukherji M, Metzen E, Wilson MI, Dhanda A, Tian YM, Masson N, Hamilton DL, Jaakkola P, Barstead R, Hodgkin J, Maxwell PH, Pugh CW, Schofield CJ, Ratcliffe PJ. C. elegans EGL-9 and mammalian homologs define a family of dioxygenases that regulate HIF by prolyl hydroxylation. *Cell* 2001;**107**:43–54.
9. Xie L, Xiao K, Whalen EJ, Forrester MT, Freeman RS, Fong G, Gygi SP, Lefkowitz RJ, Stamler JS. Oxygen-regulated beta(2)-adrenergic receptor hydroxylation by EGLN3 and ubiquitylation by pVHL. *Sci Signal* 2009;**2**:ra33.
10. Aragones J, Fraisl P, Baes M, Carmeliet P. Oxygen sensors at the crossroad of metabolism. *Cell Metab* 2009;**9**:11–22.
11. Boulahbel H, Duran RV, Gottlieb E. Prolyl hydroxylases as regulators of cell metabolism. *Biochem Soc Trans* 2009;**37**:291–294.
12. Bardella C, Pollard PJ, Tomlinson I. SDH mutations in cancer. *Biochim Biophys Acta* 2011;**1807**:1432–1443.
13. Singleton RS, Liu-Yi P, Formenti F, Ge W, Sekirnik R, Fischer R, Adam J, Pollard PJ, Wolf A, Thalhammer A, Loenarz C, Flashman E, Yamamoto A, Coleman ML, Kessler BM, Wappner P, Schofield CJ, Ratcliffe PJ, Cockman ME. OGFOD1 catalyzes prolyl hydroxylation of RPS23 and is involved in translation control and stress granule formation. *Proc Natl Acad Sci USA* 2014;**111**:4031–4036.
14. Katz MJ, Acevedo JM, Loenarz C, Galagovsky D, Liu-Yi P, Perez-Pepe M, Thalhammer A, Sekirnik R, Ge W, Melani M, Thomas MG, Simonetta S, Boccaccio GL, Schofield CJ, Cockman ME, Ratcliffe PJ, Wappner P. Sudestada1, a Drosophila ribosomal prolyl-hydroxylase required for mRNA translation, cell homeostasis, and organ growth. *Proc Natl Acad Sci USA* 2014;**111**:4025–4030.
15. Loenarz C, Sekirnik R, Thalhammer A, Ge W, Spivakovsky E, Mackeen MM, McDonough MA, Cockman ME, Kessler BM, Ratcliffe PJ, Wolf A, Schofield CJ. Hydroxylation of the eukaryotic ribosomal decoding center affects translational accuracy. *Proc Natl Acad Sci USA* 2014;**111**:4019–4024.
16. Saito K, Adachi N, Koyama H, Matsushita M. OGFOD1, a member of the 2-oxoglutarate and iron dependent dioxygenase family, functions in ischemic signaling. *FEBS Lett* 2010;**584**:3340–3347.
17. Luo W, Lin B, Wang Y, Zhong J, O'Meally R, Cole RN, Pandey A, Levchenko A, Semenza GL. PHD3-mediated prolyl hydroxylation of nonmuscle actin impairs polymerization and cell motility. *Mol Biol Cell* 2014;**25**:2788–2796.
18. Arsenault PR, Heaton-Johnson KJ, Li LS, Song D, Ferreira VS, Patel N, Master SR, Lee FS. Identification of prolyl hydroxylation modifications in mammalian cell proteins. *Proteomics* 2015;**15**:1259–1267.
19. Burridge PW, Matsa E, Shukla P, Lin ZC, Churko JM, Ebert AD, Lan F, Diecke S, Huber B, Mordwinkin NM, Plews JR, Abilez OJ, Cui B, Gold JD, Wu JC. Chemically defined generation of human cardiomyocytes. *Nat Methods* 2014;**11**:855–860.
20. Cambridge SB, Gnad F, Nguyen C, Bermejo JL, Kruger M, Mann M. Systems-wide proteomic analysis in mammalian cells reveals conserved, functional protein turnover. *J Proteome Res* 2011;**10**:5275–5284.
21. Jovanovic M, Rooney MS, Mertins P, Przybylski D, Chevrier N, Satija R, Rodriguez EH, Fields AP, Schwartz S, Raychowdhury R, Mumbach MR, Eisenhaure T, Rabani M, Gennert D, Lu D, Delorey T, Weissman JS, Carr SA, Hacohen N, Regev A. Immunogenetics. Dynamic profiling of the protein life cycle in response to pathogens. *Science* 2015;**347**:1259038.
22. Mole DR, Schlemminger I, McNeill LA, Hewitson KS, Pugh CW, Ratcliffe PJ, Schofield CJ. 2-oxoglutarate analogue inhibitors of HIF prolyl hydroxylase. *Bioorg Med Chem Lett* 2003;**13**:2677–2680.
23. McDonough MA, McNeill LA, Tilliet M, Papamicael CA, Chen QY, Banerji B, Hewitson KS, Schofield CJ. Selective inhibition of factor inhibiting hypoxia-inducible factor. *J Am Chem Soc* 2005;**127**:7680–7681.
24. Milkiewicz M, Pugh CW, Egginton S. Inhibition of endogenous HIF inactivation induces angiogenesis in ischaemic skeletal muscles of mice. *J Physiol* 2004;**560**:21–26.
25. Beers J, Linask KL, Chen JA, Siniscalchi LI, Lin Y, Zheng W, Rao M, Chen G. A cost-effective and efficient reprogramming platform for large-scale production of integration-free human induced pluripotent stem cells in chemically defined culture. *Sci Rep* 2015;**5**:11319.
26. Vizcaino JA, Csordas A, Del-Toro N, Dianes JA, Griss J, Lavidas I, Mayer G, Perez-Riverol Y, Reisinger F, Ternent T, Xu QW, Wang R, Hermjakob H. 2016 update of the PRIDE database and its related tools. *Nucleic Acids Res* 2016;**44**:D447–D456.
27. Wang G, Wu WW, Zeng W, Chou CL, Shen RF. Label-free protein quantification using LC-coupled ion trap or FT mass spectrometry: reproducibility, linearity, and application with complex proteomes. *J Proteome Res* 2006;**5**:1214–1223.
28. Pandit S, Zhou Y, Shiue L, Coutinho-Mansfield G, Li H, Qiu J, Huang J, Yeo GW, Ares M Jr, Fu XD. Genome-wide analysis reveals SR protein cooperation and competition in regulated splicing. *Mol Cell* 2013;**50**:223–235.
29. Sanford JR, Wang X, Mort M, Vanduyn N, Cooper DN, Mooney SD, Edenberg HJ, Liu Y. Splicing factor SFRS1 recognizes a functionally diverse landscape of RNA transcripts. *Genome Res* 2009;**19**:381–394.
30. Xie L, Pi X, Mishra A, Fong G, Peng J, Patterson C. PHD3-dependent hydroxylation of HCLK2 promotes the DNA damage response. *J Clin Invest* 2012;**122**:2827–2836.
31. Cockman ME, Webb JD, Kramer HB, Kessler BM, Ratcliffe PJ. Proteomics-based identification of novel factor inhibiting hypoxia-inducible factor (FIH) substrates indicates widespread asparaginyl hydroxylation of ankyrin repeat domain-containing proteins. *Mol Cell Proteomics* 2009;**8**:535–546.
32. Lam MP, Wang D, Lau E, Liem DA, Kim AK, Ng DC, Liang X, Bleakley BJ, Liu C, Tabaraki JD, Cadeiras M, Wang Y, Deng MC, Ping P. Protein kinetic signatures of the remodeling heart following isoproterenol stimulation. *J Clin Invest* 2014;**124**:1734–1744.
33. Mordwinkin NM, Burridge PW, Wu JC. A review of human pluripotent stem cell-derived cardiomyocytes for high-throughput drug discovery, cardiotoxicity screening, and publication standards. *J Cardiovasc Transl Res* 2013;**6**:22–30.
34. Fahling M. Surviving hypoxia by modulation of mRNA translation rate. *J Cell Mol Med* 2009;**13**:2770–2779.
35. Wehner KA, Schutz S, Sarnow P. OGFOD1, a novel modulator of eukaryotic translation initiation factor 2alpha phosphorylation and the cellular response to stress. *Mol Cell Biol* 2010;**30**:2006–2016.
36. Heusch G, Schulz R, Rahimtoola SH. Myocardial hibernation: a delicate balance. *Am J Physiol Heart Circ Physiol* 2005;**288**:H984–H999.
37. Steenbergen C, Deleeuw G, Rich T, Williamson JR. Effects of acidosis and ischemia on contractility and intracellular pH of rat heart. *Circ Res* 1977;**41**:849–858.
38. Carissimi C, Baccon J, Straccia M, Chiarella P, Maiolica A, Sawyer A, Rappsilber J, Pellizzoni L. Unrip is a component of SMN complexes active in snRNP assembly. *FEBS Lett* 2005;**579**:2348–2354.
39. Grimmler M, Otter S, Peter C, Muller F, Chari A, Fischer U. Unrip, a factor implicated in cap-independent translation, associates with the cytosolic SMN complex and influences its intracellular localization. *Hum Mol Genet* 2005;**14**:3099–3111.
40. Wang RS, Oldham WM, Loscalzo J. Network-based association of hypoxia-responsive genes with cardiovascular diseases. *New J Phys* 2014;**16**:105014.
41. Cottrill KA, Chan SY, Loscalzo J. Hypoxamirs and mitochondrial metabolism. *Antioxid Redox Signal* 2014;**21**:1189–1201.
42. Gao G, Dudley SC Jr. RBM25/LUC7L3 function in cardiac sodium channel splicing regulation of human heart failure. *Trends Cardiovasc Med* 2013;**23**:5–8.
43. Boeckel JN, Guarani V, Koyanagi M, Roexe T, Lengeling A, Schermuly RT, Gellert P, Braun T, Zeiher A, Dimmeler S. Jumonji domain-containing protein 6 (Jmjd6) is required for angiogenic sprouting and regulates splicing of VEGF-receptor 1. *Proc Natl Acad Sci USA* 2011;**108**:3276–3281.
44. Callapina M, Zhou J, Schnitzer S, Metzen E, Lohr C, Deitmer JW, Brune B. Nitric oxide reverses desferrioxamine- and hypoxia-evoked HIF-1alpha accumulation—implications for prolyl hydroxylase activity and iron. *Exp Cell Res* 2005;**306**:274–284.
45. Yan H, Zhang DX, Shi X, Zhang Q, Huang YS. Activation of the prolyl-hydroxylase oxygen-sensing signal cascade leads to AMPK activation in cardiomyocytes. *J Cell Mol Med* 2012;**16**:2049–2059.
46. Shen X, Wan C, Ramaswamy G, Mavalli M, Wang Y, Duvall CL, Deng LF, Guldberg RE, Eberhart A, Clemens TL, Gilbert SR. Prolyl hydroxylase inhibitors increase

neoangiogenesis and callus formation following femur fracture in mice. *J Orthop Res* 2009;**27**:1298–1305.
47. Wright G, Higgin J, Raines RT, Steenbergen C, Murphy E. Activation of the prolyl hydroxylase oxygen-sensor results in induction of GLUT1, heme oxygenase-1, and nitric-oxide synthase proteins and confers protection from metabolic inhibition to cardiomyocytes. *J Biol Chem* 2003;**278**:20235–20239.
48. Rahman SU, Lee MS, Baek JH, Ryoo HM, Woo KM. The prolyl hydroxylase inhibitor dimethyloxalylglycine enhances dentin sialophoshoprotein expression through VEGF-induced Runx2 stabilization. *PLoS One* 2014;**9**:e112078.
49. Zhdanov AV, Okkelman IA, Collins FW, Melgar S, Papkovsky DB. A novel effect of DMOG on cell metabolism: direct inhibition of mitochondrial function precedes HIF target gene expression. *Biochim Biophys Acta* 2015;**1847**:1254–1266.